

Si and Be intralayers at GaAs/AlAs and GaAs/GaAs junctions: Low-temperature photoemission measurements

M. Moreno,* M. Alonso, and J. L. Sacedón

Instituto de Ciencia de Materiales de Madrid (CSIC), Cantoblanco, E-28049 Madrid, Spain

M. Hörnicke and R. Hey

Paul-Drude-Institut für Festkörpelelektronik, Hausvogteiplatz 5-7, D-10117 Berlin, Germany

K. Horn

Fritz-Haber-Institut der Max-Planck-Gesellschaft, Faradayweg 4-6, D-14195 Berlin, Germany

K. H. Ploog

Paul-Drude-Institut für Festkörpelelektronik, Hausvogteiplatz 5-7, D-10117 Berlin, Germany

(Received 29 November 1999)

In order to distinguish between conflicting interpretations regarding the effect of intralayer insertion at semiconductor junctions, we have carried out synchrotron-radiation photoemission studies of GaAs/AlAs(100) heterojunctions and GaAs/GaAs(110) homojunctions, with and without a Si or a Be intralayer, at room temperature and at low temperature. The synchrotron light induces photovoltage effects at low temperature, which are found to be consistent with the room-temperature band profiles we have previously proposed for these heterojunctions [M. Moreno *et al.*, Phys. Rev. B **58**, 13 767 (1998)], assuming a doping role for the intralayer atoms. Band discontinuities play an important role in determining the type of photovoltage effects induced. Our experimental observations can be fully understood in terms of intralayer-induced changes of the band-bending profile, and the occurrence of photovoltage effects at low temperature, calling into question the previous interpretation of room-temperature photoemission results from GaAs/AlAs heterojunctions in terms of intralayer-induced “band-offset” changes.

I. INTRODUCTION

Photoemission spectroscopy (PES) is extensively used to determine valence-band discontinuities (ΔE_V) at semiconductor heterojunctions. The offset is typically obtained from the separation of shallow core levels in the buried layer and the overlayer, assuming that bands are flat along the photoemission probing depth.¹⁻⁶ This “flatband condition” is generally fulfilled, and disturbing effects — such as for instance the existence of chemical shifts — are usually not important, or can be quantified. Hence, the band offset measured by PES, which we term the “apparent” discontinuity, often closely approaches the real offset. However, for heterostructures with complex interfacial arrangements, the assumption of flatband conditions can lead to serious errors in band-offset determinations by PES.

An intriguing concept that has stimulated an intense research effort is that of “band-offset engineering,” i.e., the intentional modification of band offsets through the introduction of about-monolayer quantities of foreign atoms.⁷ Sorba and co-workers⁸⁻¹¹ studied the insertion of a thin Si layer at AlAs-GaAs interfaces, and found significant changes of the apparent valence-band discontinuity, as measured by PES, which they interpreted as real band-offset changes, assuming flatband conditions. This interpretation⁸⁻¹¹ was questioned by several groups,¹²⁻¹⁵ who invoked the doping role of Si atoms in III-V semiconductors.^{16,17} They argued that Si insertion induces a non-negligible band bending within the photoemission probing depth, resulting in an “apparent”

change of the band offset measured by PES, which does not correspond to a “real” modification of the interface band discontinuity. Taking into account the *n*-type (*p*-type) doping role of Si (Be) impurities in III-V semiconductors,¹⁶ we have shown¹⁵ that the changes of the apparent valence-band offset observed upon Si or Be insertion at GaAs/AlAs heterojunctions can be successfully explained just by considering the intralayer-induced variations of the band-bending potential, without including any change of the interface valence-band offset. Here we present additional support for this alternative interpretation in terms of “band-bending changes.”

In order to accurately determine band discontinuities by photoemission, it is mandatory to perform the experiment under ideal *flatband* conditions. Surface photovoltage (SPV) effects have been shown to produce steady-state conditions in which the band bending is reduced or eliminated.¹⁸⁻³¹ In particular, SPV effects can be induced by the synchrotron light sometimes used to excite photoelectrons in PES measurements.²¹⁻³³ For the simplest case, involving a homogeneous semiconductor material, the process can be viewed as follows. Soft x-ray photons excite electrons to the conduction band, leaving holes in the valence band or core levels; secondary excitations and nonradiative decay processes effectively multiply the number of charge carriers.³²⁻³⁸ Electrons and holes are accelerated in opposite directions (photocurrent) by the built-in field present in the semiconductor depletion region, so that minority carriers accumulate at the surface. This carrier separation produces a photovoltage

(SPV) which opposes the initial built-in voltage.^{32,33} In order to maintain a charge balance, a current of majority carriers flows to the surface (restoring current).^{27,28,30,32,33} In equilibrium, the restoring current is equivalent and opposite to the photocurrent, so that both currents cancel each other. The supply of the restoring current is limited by the depletion-region resistance, which has a pronounced dependence on sample temperature. At room temperature (RT), the restoring current is usually sufficient to quickly discharge most of the induced photovoltage.¹⁹ However, at low temperature the restoring currents are reduced and there is a net forward bias.^{19,21–25,32,33} The magnitude of the photovoltage depends on the doping density and band-gap value of the sample,^{24,27,29,30,32,33} and on features of the photon source, such as illumination intensity, time structure, etc.^{27,28,32,33,39,40} Larger SPV values are achieved for lower doping densities, and wider band-gap values. The surface photovoltage tends to reduce, eventually to zero, any initial band bending present at the surface. Hence it has the effect of flattening the surface potential barrier. As a result, the valence and core-level PES signals are shifted toward their unpinned energy positions.^{19,21,22,25,30}

The saturation photovoltage induced by synchrotron radiation (SR) at low temperature was used by Yu *et al.*⁴¹ to measure the band offset at CdTe/GaAs(110) heterojunctions under flatband conditions. These results showed that the sharp variation of the electrostatic potential across the heterojunction remains unchanged by the photovoltage, so that low-temperature photoemission can be successfully used to determine valence-band offsets under nonequilibrium steady-state flatband conditions.⁴¹ Nevertheless, this possibility of measuring band offsets at low temperature has been scarcely exploited. Here, we present synchrotron-radiation PES experiments performed at room temperature and at low temperature on GaAs/AlAs(100) heterojunctions and GaAs/GaAs(110) homojunctions, without and with a Si or a Be intralayer. Our aim is to analyze the consistency of the band profiles that we have previously proposed¹⁵ for GaAs/AlAs(100), GaAs/Si/AlAs(100), and GaAs/Be/AlAs(100) heterojunctions at room temperature, with the experimental behavior observed at low temperature. We investigate the SPV effects induced upon cooling, and discuss some of their peculiarities in heterojunctions, which are important to determine band offsets through low-temperature PES measurements.

II. EXPERIMENT

Using molecular-beam epitaxy (MBE), we have grown (i) GaAs/AlAs heterojunctions, and (ii) GaAs/GaAs homojunctions, on epitaxially heavily Si-doped ($n = 1 \times 10^{18} \text{ cm}^{-3}$) GaAs (100)-[2° off toward (111)A] and (110) substrates, respectively. A (0.1–0.3)- μm -thick Si-doped ($n = 1 \times 10^{18} \text{ cm}^{-3}$) GaAs buffer layer was first grown, followed by a 20.0-nm-thick undoped AlAs (or GaAs) layer. A layer of Si or Be, with a density of $2.2 \times 10^{14} \text{ atoms cm}^{-2}$ [corresponding to approximately 1/3 of the atomic sites in a (100) monolayer], was then inserted in some of the samples using a *pulsed low-flux* δ -doping method.^{42,43} Finally, all samples were terminated by a 2.0-nm-thick, nominally undoped, GaAs overlayer. Details on

the growth parameters can be found in Refs. 14 and 15.

After growth, the samples were transferred under ultra-high vacuum from the MBE chamber to the PES station at the synchrotron source, by using a small transfer chamber. The samples were placed together in the analysis chamber, under electrical contact and grounded. We used a multiple sample holder which accommodated several samples. One ‘‘special’’ holder position was designed to be in thermal contact with a liquid-N₂ reservoir. The low-temperature measurements were carried out by placing the sample to be analyzed in this cooling position. The temperature at which the samples were cooled down in this way is called ‘‘low temperature,’’ and denoted LT in the following. It corresponds to a thermocouple reading of 220 K. Equal LT conditions were reproducibly obtained with this cooling arrangement, the actual temperature being probably lower than the nominal.

The samples were analyzed by PES, immediately after growth, using synchrotron radiation coming from the TGM6 beamline of BESSY I (*Berliner Elektronenspeicherring-Gesellschaft für Synchrotronstrahlung mbH*). The TGM6 monochromator was located in front of a wiggler/undulator, and delivered 10^{12} – 10^{13} photons/s in the photon energy range used. Electron kinetic-energy distribution curves (EDC’s) were obtained for each sample at both room and low temperatures. We recorded the Ga(3*d*), [Al(2*p*)], and valence-band-edge emissions on GaAs/AlAs heterojunctions and on GaAs/GaAs homojunctions, using 95- and 40-eV photons, respectively. These photon energies were selected because they excite photoelectrons in the buried layer up to a kinetic energy of ~ 15 eV, for which the electron mean free path is relatively long. In order to have a common energy reference for the measurements performed in the different samples, we recorded the Fermi-edge emission from a gold foil that was in electrical contact with the back side of the semiconductor samples. Electrons were collected and counted in normal-emission geometry by an angle-resolving photoelectron spectrometer. The overall energy resolution was 150–300 meV in the range of photon energies used.

III. RESULTS

A. Heterojunctions

Figure 1 shows Al(2*p*), Ga(3*d*), and valence-band-edge photoelectron kinetic-energy spectra recorded at room and at low temperatures, on three types of GaAs-on-AlAs(100) heterostructures: (a) without any intralayer, (b) with a Si intralayer, and (c) with a Be intralayer. The figure also shows Fermi-edge spectra recorded on gold, which permit a determination of the kinetic energy corresponding to the Fermi level (E_F) deep in the bulk of the semiconductor samples ($E_k = 90$ eV, see the dotted line). This is a reference energy for all the spectra shown in Fig. 1. Note that due to the high *n*-type doping level of the substrates, E_F lies close to the conduction-band minimum (CBM) deep in the bulk of all our samples. The LT signals from the GaAs/AlAs(100) and GaAs/Be/AlAs(100) heterostructures appear *significantly shifted* relative to the RT emissions (Fig. 1). The sign of the shifts is the same in these two cases. Moreover, the Al(2*p*), Ga(3*d*) and valence-band-edge signals shift *rigidly* for both

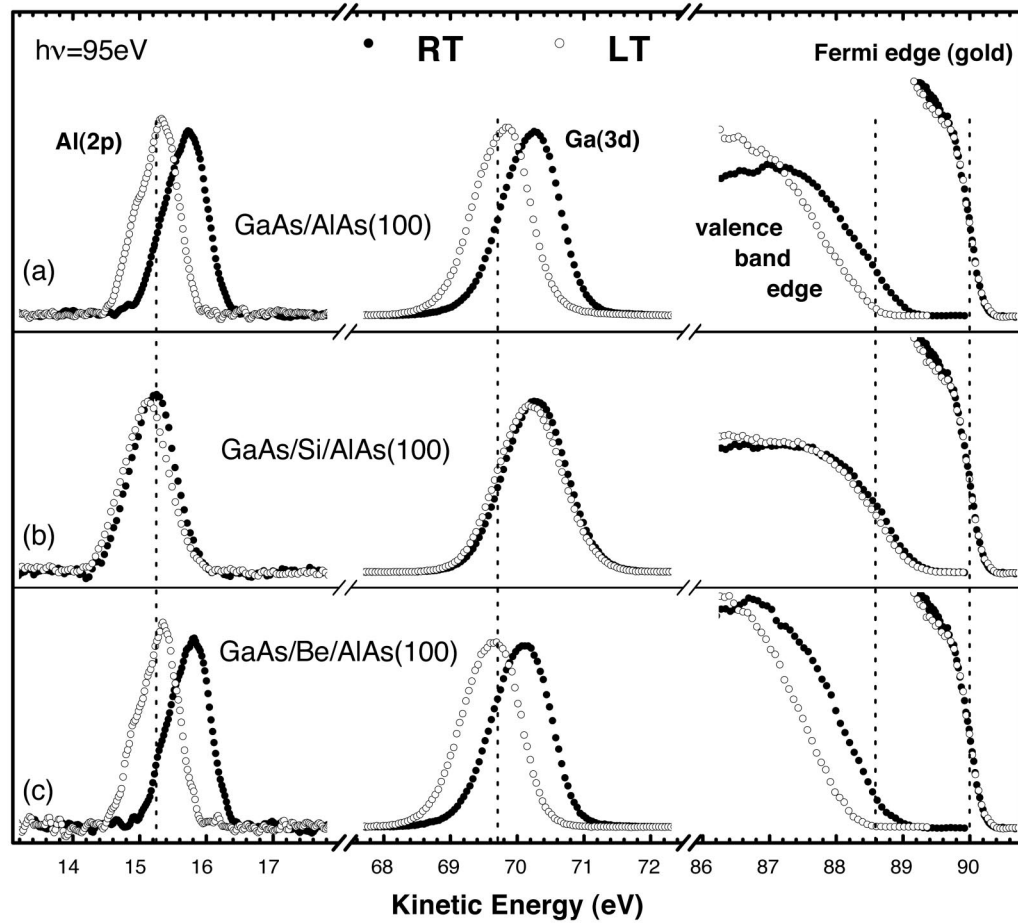


FIG. 1. Al($2p$), Ga($3d$) and valence-band-edge EDC spectra recorded with 95-eV photons at room temperature (solid circles), and at low temperature $T \sim 220$ K (open circles) on (a) GaAs/AlAs(100), (b) GaAs/Si/AlAs(100), and (c) GaAs/Be/AlAs(100) heterostructures. Fermi-edge spectra recorded on a gold foil in electrical contact with the back side of the semiconductor samples. The intensity has been normalized. The vertical dotted lines mark the kinetic-energy positions corresponding to the Al($2p$), Ga($3d$) and valence-band-maximum levels under “flatband conditions,” as well to the “bulk” Fermi level.

types of samples; shifts of 0.43 and 0.47 eV toward lower kinetic energies are measured for the GaAs/AlAs(100) and GaAs/Be/AlAs(100) heterostructures, respectively. In contrast, for the GaAs/Si/AlAs(100) heterostructure the PES signals *scarcely shift* upon cooling (< 0.1 eV).

PES reports on “band-offset modifications”⁸ carefully analyze any variation in the Al($2p$)-to-Ga($3d$) energy separation, which is considered to be the relevant parameter. In order to highlight even small changes of this separation or/and of the core-level line shapes upon cooling, the Al($2p$) and Ga($3d$) signals have been represented in Fig. 2 on a *relative binding-energy* scale, so that the common energy reference for the spectra is the *surface* valence-band maximum (VBM), instead of the bulk Fermi level. Each data set [Al($2p$), Ga($3d$), and valence-band-edge spectra] was rigidly shifted up to align the leading edges of all the valence-band spectra; hence the different energy positions of the surface VBM (for the different samples and temperatures) in the kinetic-energy scale of Fig. 1 are brought to coincidence in the binding-energy scale of Fig. 2. The zero of this binding-energy scale has been arbitrarily chosen at the centroid position of the Ga($3d$) peak measured at RT on the GaAs/AlAs(100) heterostructure without intralayer (the “centroid” being defined as the energy value that divides the peak into two parts with equal area).

Figure 2 unambiguously shows that the Al($2p$)-to-Ga($3d$) energy separation measured for each sample at LT is *identical* to that measured at RT.⁴⁴ Reducing the sample temperature does not produce any significant modification of the Al($2p$) and Ga($3d$) line shapes either. The core-level line shapes are not modified upon Be insertion, while they are broadened toward higher binding energies upon Si insertion.^{14,15} As a consequence, the centroid of the Ga($3d$) peak from GaAs/Be/AlAs(100) coincides in Fig. 2 with that from GaAs/AlAs(100), whereas the Ga($3d$) centroid from GaAs/Si/AlAs(100) is slightly shifted toward higher binding energy.

Several effects can modify the Al($2p$)-to-Ga($3d$) energy separation measured by PES on GaAs/AlAs heterojunctions, upon intralayer insertion. The origin most frequently invoked for such changes is a modification of the heterojunction band offset,^{8,9,11,45} but a variation of the overlayer band bending can also lead to a change in the core-level separation.¹⁵ Since in our experiment the Al($2p$)-to-Ga($3d$) separation does not change upon cooling (Fig. 2), we conclude that neither the heterojunction band offset nor the overlayer band bending are modified.⁴⁶ The absence of band-offset changes upon cooling can be reasonably expected.⁴⁷ What seems more noticeable, and deserves a further comment below, is the ab-

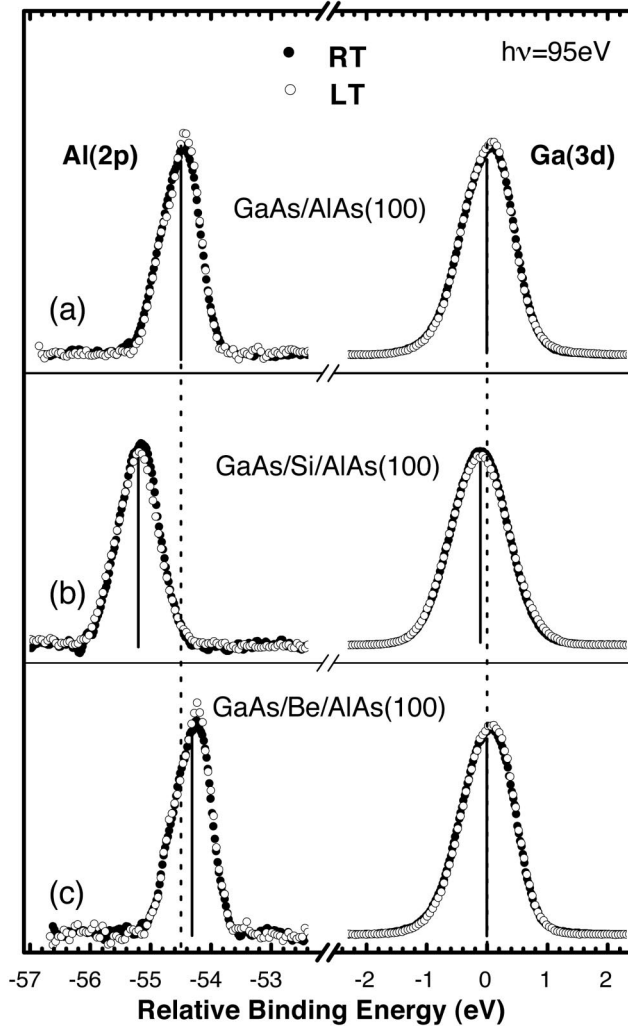


FIG. 2. Al($2p$) and Ga($3d$) spectra of Fig. 1 represented in a relative binding-energy scale, where the energy positions of the surface VBM are coincident. The centroid positions of the different peaks are marked by solid lines.

sence of changes in the overlayer band bending upon cooling.

The rigidity of the shifts shown in Fig. 1, and the absence of core-level line-shape changes upon cooling suggest that these shifts have an electronic origin rather than a chemical one. They can be readily explained through the occurrence of photoinduced nonequilibrium processes at low temperature, which modify the RT band profiles. Photovoltage effects may be induced in those regions of the sample where light penetrates; they can in principle occur in the GaAs overlayer, the AlAs buried layer, and even in a portion of the n -GaAs substrate. In our discussion we will assume, for RT, the band profiles that we have previously proposed,¹⁵ which are represented in Fig. 3 by solid lines. We show below that the experimental results of Figs. 1 and 2 can be completely understood by considering light-induced modifications of these RT band profiles, so that at LT bands become completely flat in the AlAs region, and the band bending in the GaAs overlayer remains unchanged (see the LT profiles displayed in Fig. 3 as dotted lines).

Let us first analyze the band-profile variations in the AlAs region of the samples. Because of the small escape depth of

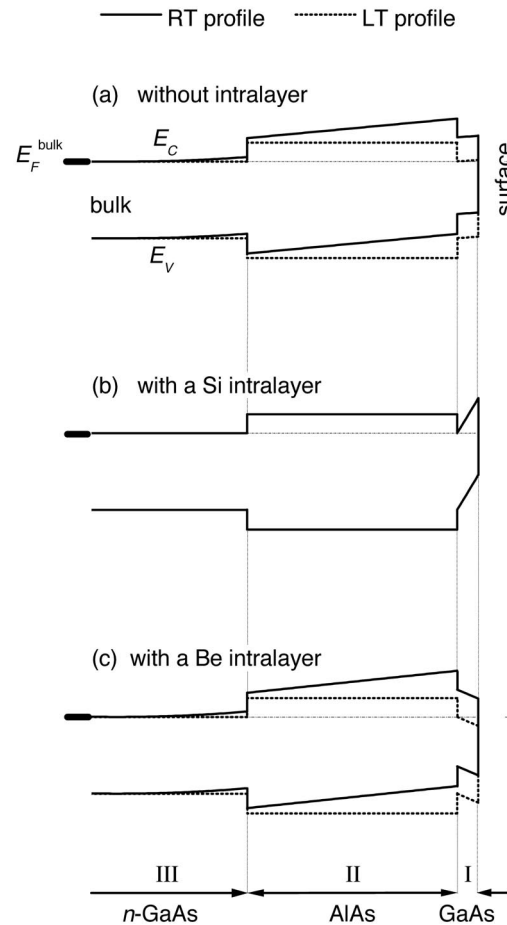


FIG. 3. Band profiles proposed for (a) GaAs/AlAs(100), (b) GaAs/Si/AlAs(100), and (c) GaAs/Be/AlAs(100) heterostructures, when illuminated with 95-eV photons at room temperature (solid lines) and at low temperature (dotted lines). The thin dash-dotted horizontal lines mark the position of the Fermi level *deep in the bulk* of the samples.

the photoelectrons, the Al($2p$) signal mostly originates in a shallow thin portion of the AlAs layer, close to the front AlAs-GaAs interface.¹⁵ Hence the energy of this peak reflects the value of the band-bending potential at this position in the sample. According to the profile proposed for the GaAs/Si/AlAs(100) heterostructure at RT [solid lines in Fig. 3(b)], the bands are flat along the AlAs buried layer. Thus, *a priori*, there is no reason for the induction of a photovoltage in this region. This explains why the Al($2p$) signal from the Si-containing sample scarcely moves upon cooling [Fig. 1(b)]. Conversely, the RT band profiles proposed for the GaAs/AlAs(100) and GaAs/Be/AlAs(100) heterostructures indicate the existence of an *upward* band bending along the AlAs region [see Figs. 3(a) and 3(c)]. Thus a photovoltage can be established at LT, producing a band flattening in the AlAs layer, and consequently a shift of the Al($2p$) signal toward *lower* kinetic energies, as observed experimentally [Figs. 1(a) and 1(c)].

The kinetic energy expected for the Al($2p$) level, if the bands were completely flat all along the n -GaAs substrate and the AlAs buried layer, in any of the GaAs/AlAs/ n -GaAs(100) heterostructures, is marked in Fig. 1 by a vertical dotted line, and corresponds to a value E_k

=15.24 eV.⁴⁸ Figure 1 shows that the Al(2*p*) peaks measured at LT on the three types of heterostructures approximately converge on a common energy position, which is very close to the “flatband” energy. The agreement with the flatband position is very good for the heterostructures without any intralayer and with a Be intralayer [the corresponding Al(2*p*) centroids appear at kinetic energies of 15.28 and 15.29 eV, respectively]. For the Si-containing heterostructure, the LT Al(2*p*) centroid (at 15.09 eV) is slightly shifted toward lower kinetic energies relative to the flatband energy. This is probably due to the Si-induced modification of the Al(2*p*) line shape,^{14,15} which slightly changes the position of the peak centroid. Hence, upon illumination with synchrotron radiation at LT, the bands are seen to approximately reach the so-called flatband energy at the position of the front AlAs-GaAs interface (AlAs side) for the three types of heterostructures, and it is reasonable to conclude that the bands become completely flat down to the deep *n*-GaAs bulk, as depicted in Fig. 3 (dotted lines).

The Ga(3*d*) signal mostly originates in a very thin GaAs layer close to the sample surface.¹⁵ Hence the energy of this peak reflects the value of the band-bending potential *at the sample surface*. The energy position of the VBM at the surface (relative to the energy position of the Fermi level deep in the bulk) can be derived from the Ga(3*d*) peak, or directly from the valence-band-edge spectrum. In a *hypothetical* situation where the bands would be completely flat all along the GaAs/AlAs/*n*-GaAs(100) heterostructures, the Ga(3*d*) and valence-band-edge emissions would appear in the PES spectra at kinetic energies $E_k[\text{Ga}(3d)]=69.71$ eV and $E_k[\text{VBM}]=88.57$ eV, respectively, assuming a *constant band-offset value* upon intralayer insertion.⁴⁹ Such “flatband energy positions” are marked in Fig. 1 as vertical dotted lines. A deviation of the recorded signals from such positions indicates the existence of band bending, provided that the occurrence of chemical shifts or/and band-offset changes is discarded.

The Ga(3*d*) and valence-band-edge signals have been observed to shift upon cooling by *exactly* the same amount than the corresponding Al(2*p*) signals (Fig. 1). The constancy of the Al(2*p*)-to-Ga(3*d*) energy separation (Fig. 2) indicates that the overlayer band bending does not vary upon cooling. Therefore, the shifts of the Ga(3*d*) and valence-band-edge signals cannot be due to a light-induced flattening of the bands in the GaAs overlayer. However, such shifts can be well understood as being a consequence of the flattening of the AlAs bands, which additionally causes the bands in the GaAs overlayer to be rigidly “pulled down” toward higher binding energies (as depicted in Fig. 3), such that the Ga(3*d*) and valence-band-edge signals are shifted toward lower kinetic energies.⁵⁰

In principle, by reducing the sample temperature, one would expect the occurrence of SPV effects in those illuminated regions of the semiconductor where there is band bending at RT. Therefore, at first glance it may appear striking not to observe any change of the band bending in the GaAs overlayer, for any of the samples, not even for the GaAs/Si/AlAs(100) heterostructure where, according to the profile that we have proposed [Fig. 3(b)], a sharp band bending exists in the GaAs overlayer at RT. This result is in contrast with that reported by Yu *et al.*⁴¹ for CdTe/

GaAs(110) heterojunctions, where a light-induced band flattening in *both* the CdTe overlayer and the GaAs substrate was found, upon cooling the sample down to 35 K. The persistence of the overlayer band bending in our samples upon cooling can be explained by taking into account our particular experimental conditions. Two aspects are *a priori* relevant: (i) the SPV dependence on temperature,^{19,24,25,32} and (ii) the role played by the interface band offsets.⁵¹

The persistence of the overlayer band bending might be due to the particular “low” temperature used [note that our “low” temperature is higher than the temperature of 35 K used in the experiments on CdTe/GaAs(110)].⁴¹ Since non-equilibrium effects are more favorable in AlAs than in GaAs (because of the larger and indirect AlAs band gap), the “low” temperature we used might permit a photovoltage to be maintained in the AlAs region, but not in the GaAs overlayer. Another explanation for the band-bending persistence in the overlayer might relate to the type of stacking sequence of our samples: the material with the narrower band gap, GaAs, has been grown on top of the material with the wider band gap, AlAs. For this type of stacking sequence, the band offsets at the front AlAs-GaAs interface act as energy barriers, preventing the transport of the photogenerated carriers through the interface. In the three heterostructures considered, these band discontinuities restrict the spatial separation of the electron-hole pairs photogenerated in the overlayer, to the thickness of the overlayer itself, which is only 2 nm. The overlap of the electron and hole wave functions inside this thin layer is considerable (the Bohr radius of the free electrons is ~ 10 nm and that of the free holes is ~ 3 nm). Therefore, the recombination rate is high, and the establishment of a photovoltage in the overlayer region is ineffective. Hence the band discontinuities existing at the AlAs-GaAs interface may play a relevant role in determining the type of SPV effects occurring in our samples.

B. Homojunctions

Photovoltage effects in homojunctions may be quite different from those occurring in heterojunctions, because in homojunctions there are no band offsets preventing the transport of carriers across the sample. Figure 4 compares Ga(3*d*) spectra recorded at room temperature and at low temperature on GaAs(110) and GaAs/Si/GaAs(110) samples. The spectra are referenced to the position of the Fermi level deep in the bulk of the samples, which appears at a kinetic energy $E_k=35$ eV. Upon cooling, the Ga(3*d*) peaks recorded on the two types of samples shift to lower kinetic energies, converging on a common position $E_k=15.1$ eV (the vertical dotted line in Fig. 4). Shifts of 0.2 and 0.4 eV are measured for GaAs(110) and GaAs/Si/GaAs(110), respectively. The Ga(3*d*) line shape for the GaAs(110) sample is scarcely modified upon cooling; it only seems slightly better resolved at LT. The Ga(3*d*) peak recorded on the GaAs/Si/GaAs(110) homojunction at RT evidences the line-shape changes induced by Si insertion^{14,15}; upon cooling, the peak narrows significantly.

The shifts of the Ga(3*d*) emissions to *lower* kinetic energies upon cooling (Fig. 4) are consistent with a light-induced flattening of the bands that are bent *upwards* at RT.⁵² The built-in field associated with the surface band bending in the

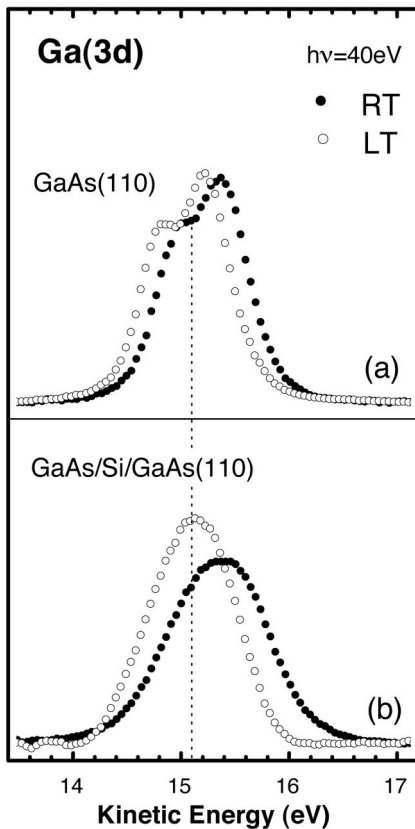


FIG. 4. Ga(3d) spectra recorded with 40-eV photons at room temperature (solid circles) and at low temperature $T \sim 220$ K (open circles) on (a) GaAs(110) and (b) GaAs/Si/GaAs(110) samples. The spectra are shown after peak-area normalization. The common position of the Ga(3d) centroids for the two samples at LT is marked by a vertical dotted line.

GaAs(110) and GaAs/Si/GaAs(110) samples at RT drives the electrons photogenerated in the overlayer toward the bulk of the sample without encountering any energy barrier, while holes accumulate at the surface. Some authors⁵³ proposed that insertion of Si at GaAs/GaAs(100) homojunctions induces a band offset; however, such an effect has not been conclusively demonstrated,¹⁴ and we will not consider it. Electrons and holes photogenerated in the GaAs overlayer of GaAs/GaAs(110) homojunctions (with and without intralayer) can separate by a much wider distance than in the case of GaAs-on-AlAs heterojunctions, so that a surface photovoltage (and a corresponding band flattening) can thus be effectively induced in the overlayer of *homojunctions*, contrary to the case of GaAs-on-AlAs *heterojunctions*.

The coincidence of the Ga(3d) peak energies at LT for GaAs(110) and GaAs/Si/GaAs(110) (Fig. 4) can be understood by considering the pronounced dependence of SPV on the sample temperature. This common position probably corresponds to the highest flattening achievable at the particular ‘‘low’’ temperature used. However, this energy position does not correspond to completely flat bands, since for flat bands the Ga(3d) peaks should have been shifted even more, to a kinetic energy $E_k = 14.7$ eV. The narrowing of the Ga(3d) peak observed for the GaAs/Si/GaAs(110) structure (Fig. 4) is also explained by the nonequilibrium processes induced at LT, which tend to eliminate peak broadenings associated

with the existence of band bending within the Ga(3d) probing depth, and/or with inhomogeneities in the pinning position of the Fermi level at the surface.^{54–56}

Important conclusions can be reached by comparing the PES results obtained under similar experimental conditions for homojunctions and heterojunctions. On the one hand we have observed a *total* band flattening in the AlAs layer of GaAs/AlAs(100) heterojunctions, and only a *partial* band flattening in the GaAs material of GaAs/GaAs(110) homojunctions. This can be understood by taking into account that the establishment of a photovoltage is more favorable in AlAs than in GaAs. On the other hand, we have observed a *nonzero* band flattening in the GaAs material of GaAs/Si/GaAs(110) *homojunctions* (Fig. 4), but a *zero* band flattening in the GaAs overlayer of GaAs/Si/AlAs(100) *heterojunctions* (Fig. 2). From this result we conclude that the specific temperature we used is not the reason for preventing the induction of a photovoltage in the GaAs overlayer of GaAs/AlAs(100) heterojunctions; instead, the band discontinuities existing at the front AlAs-GaAs interface are the main cause. Hence, in order to measure the band offset of type-I heterojunctions by PES with accuracy, the material with the wider band gap should be grown on top of the material with the narrower band gap, to allow the flattening of the overlayer bands.

IV. CONCLUSIONS

Our PES results on GaAs/AlAs(100) heterojunctions and GaAs/GaAs(110) homojunctions, with and without intralayers, can be consistently understood by considering the intralayer-induced changes of the *band-bending* profile, and the occurrence of *photovoltage* effects at low temperature. SR illumination at LT induces a complete band flattening along the *n*-GaAs substrate and the AlAs layer of the GaAs/AlAs/*n*-GaAs(100) heterojunctions, while the band bending in the GaAs overlayer remains unchanged. Such LT results are consistent with the RT band profiles that we have previously proposed,¹⁵ which were calculated assuming a *doping* role for the intralayer atoms, and a *constant* band-offset value upon intralayer insertion. Band discontinuities have been found to play an important role in determining the type of photovoltage effects induced in our samples. For instance, they prevent the flattening of the overlayer bands in GaAs-on-AlAs heterojunctions. Considering the present low-temperature results, and the room-temperature results that we previously reported on different interface geometries,¹⁴ and on intralayers with different doping behaviors,¹⁵ the ‘‘band-bending interpretation,’’^{12–15} is seen to be clearly more appropriate than the ‘‘band-offset interpretation,’’^{8–11} in describing the effect of intralayer insertion. Such results strongly question the viability of the ‘‘band-offset engineering’’ concept in III-V/III-V junctions through insertion of group-IV intralayers.

ACKNOWLEDGMENTS

We gratefully acknowledge W. Braun for the flexibility in the beam-time scheduling, necessary to coordinate the synchrotron experiments with the MBE sample growth,

H. P. Schönherr and P. Schützendübe for their expert MBE assistance, and C. Polop, S. -A. Ding, and S. Barman for technical assistance during the synchrotron beamtimes. One of us (M.M.) acknowledges the financial aid from the *Comunidad Autónoma de Madrid* (Spain). This work was partially

supported by the Spanish *Dirección General de Enseñanza Superior e Investigación Científica* under Grant Nos. PB98-524 and PB97-1195. The work at BESSY was supported by the EU Human Capital and Mobility Program under Contract No. CHGE-CT93-0027.

*Electronic address: mmoreno@icmm.csic.es

- ¹J.R. Waldrop and R.W. Grant, Phys. Rev. Lett. **43**, 1686 (1979).
- ²E.A. Kraut, R.W. Grant, J.R. Waldrop, and S.P. Kowalczyk, Phys. Rev. Lett. **44**, 1620 (1980).
- ³R.W. Grant, E.A. Kraut, S.P. Kowalczyk, and J.R. Waldrop, J. Vac. Sci. Technol. B **1**, 320 (1983).
- ⁴A.D. Katnani and G. Margaritondo, Phys. Rev. B **28**, 1944 (1983).
- ⁵J.R. Waldrop, R.W. Grant, S.P. Kowalczyk, and E.A. Kraut, J. Vac. Sci. Technol. A **3**, 835 (1985).
- ⁶F. Capasso and G. Margaritondo, *Heterojunction Band Discontinuities: Physics and Device Applications* (North-Holland, Amsterdam, 1987).
- ⁷A. Franciosi and C.G. Van de Walle, Surf. Sci. Rep. **25**, 1 (1996).
- ⁸L. Sorba, G. Bratina, G. Ceccone, A. Antonini, J.F. Walker, M. Micovic, and A. Franciosi, Phys. Rev. B **43**, 2450 (1991).
- ⁹G. Ceccone, G. Bratina, L. Sorba, A. Antonini, and A. Franciosi, Surf. Sci. **251/252**, 82 (1991).
- ¹⁰L. Sorba, G. Bratina, A. Antonini, A. Franciosi, L. Tapfer, A. Migliori, and P. Merli, Phys. Rev. B **46**, 6834 (1992).
- ¹¹A. Franciosi, L. Sorba, G. Bratina, and G. Biasiol, J. Vac. Sci. Technol. B **11**, 1628 (1993).
- ¹²M. Akazawa, H. Hasegawa, H. Tomozawa, and H. Fujikura, Jpn. J. Appl. Phys. **31**, L1012 (1992).
- ¹³Y. Hashimoto, G. Tanaka, and T. Ikoma, J. Vac. Sci. Technol. B **12**, 125 (1994).
- ¹⁴M. Moreno, H. Yang, M. Höricke, M. Alonso, J.A. Martín-Gago, R. Hey, K. Horn, J.L. Sacedón, and K.H. Ploog, Phys. Rev. B **57**, 12 314 (1998).
- ¹⁵M. Moreno, J.L. Sacedón, M. Alonso, M. Höricke, R. Hey, J. Avila, M.C. Asensio, K. Horn, and K.H. Ploog, Phys. Rev. B **58**, 13 767 (1998).
- ¹⁶E. F. Schubert, *Doping in III-V Semiconductors* (Cambridge University Press, Cambridge, 1993).
- ¹⁷E. F. Schubert, *Delta-Doping of Semiconductors* (Cambridge University Press, Cambridge, 1996).
- ¹⁸A.Y. Cho and J.R. Arthur, Phys. Rev. Lett. **22**, 1180 (1969).
- ¹⁹J.E. Demuth, W.J. Thompson, N.J. DiNardo, and R. Imbihl, Phys. Rev. Lett. **56**, 1408 (1986).
- ²⁰J.P. Long, H.R. Sadeghi, J.C. Rife, and M.N. Kabler, Phys. Rev. Lett. **64**, 1158 (1990).
- ²¹M. Alonso, R. Cimino, and K. Horn, Phys. Rev. Lett. **64**, 1947 (1990).
- ²²M. Alonso, R. Cimino, C. Maierhofer, T. Chassé, W. Braun, and K. Horn, J. Vac. Sci. Technol. B **8**, 955 (1990).
- ²³S. Chang, I.M. Vitomirov, L.J. Brillson, D.F. Rioux, P.D. Kirchner, G.D. Pettit, J.M. Woodall, and M.H. Hecht, Phys. Rev. B **41**, 12 299 (1990).
- ²⁴D. Mao, A. Kahn, M. Marsi, and G. Margaritondo, Phys. Rev. B **42**, 3228 (1990).
- ²⁵M. Alonso, R. Cimino, and K. Horn, J. Vac. Sci. Technol. A **9**, 891 (1991).
- ²⁶T.U. Kampen, D. Troost, X.Y. Hou, L. Koenders, and W. Mönch, J. Vac. Sci. Technol. B **9**, 2095 (1991).
- ²⁷A. Bauer, M. Prietsch, S. Molodtsov, C. Laubschat, and G. Kaindl, J. Vac. Sci. Technol. B **9**, 2108 (1991).
- ²⁸D.A. Evans, T.P. Chen, T. Chassé, and K. Horn, Appl. Surf. Sci. **56-58**, 233 (1992).
- ²⁹R. Cimino, A. Giarante, M. Alonso, and K. Horn, Appl. Surf. Sci. **56-58**, 151 (1992).
- ³⁰K. Horn, M. Alonso, and R. Cimino, Appl. Surf. Sci. **56-58**, 271 (1992).
- ³¹D. Mao, M. Santos, M. Shayegan, A. Kahn, G. Le Lay, Y. Hwu, G. Margaritondo, L.T. Florez, and J.P. Harbison, Phys. Rev. B **45**, 1273 (1992).
- ³²M.H. Hecht, Phys. Rev. B **41**, 7918 (1990).
- ³³M.H. Hecht, J. Vac. Sci. Technol. B **8**, 1018 (1990).
- ³⁴E.D. Johnson, Phys. Rev. **111**, 153 (1958).
- ³⁵J. Tauc, *Photo and Thermoelectric Effects in Semiconductors* (Pergamon, New York, 1962).
- ³⁶J. Lagowski, I. Baltov, and H.C. Gatos, Surf. Sci. **40**, 216 (1973).
- ³⁷H. J. Hovel, *Solar Cells* (Academic, New York, 1975).
- ³⁸G. Margaritondo, L.J. Brillson, and N.G. Stoffel, Solid State Commun. **35**, 277 (1980).
- ³⁹R.J. Hamers and K. Markert, Phys. Rev. Lett. **64**, 1051 (1990).
- ⁴⁰M.H. Hecht, Phys. Rev. B **43**, 12 102 (1991).
- ⁴¹X. Yu, A. Raisanen, G. Haugstad, G. Ceccone, N. Troullier, and A. Franciosi, Phys. Rev. B **42**, 1872 (1990).
- ⁴²L. Däweritz, H. Kostial, R. Hey, M. Ramsteiner, J. Wagner, M. Maier, J. Behrend, and M. Höricke, J. Cryst. Growth **150**, 214 (1995).
- ⁴³K.H. Ploog and L. Däweritz, Jpn. J. Appl. Phys. **34**, 691 (1995).
- ⁴⁴As we previously reported (Refs. 14 and 15), the Al(2*p*)-to-Ga(3*d*) separation is different for each type of sample [54.50 eV for GaAs/AlAs(100), 55.09 eV for GaAs/Si/AlAs(100), and 54.31 eV for GaAs/Be/AlAs(100)], as a result of intralayer insertion.
- ⁴⁵T. Saito, Y. Hashimoto, and T. Ikoma, Phys. Rev. B **50**, 17 242 (1994).
- ⁴⁶An alternative explanation could be that both types of changes do exist, but counterbalance each other. However this possibility is highly improbable, because it requires that both effects produce shifts by exactly the same absolute value and opposite sign, and this should occur for both Si and Be insertions.
- ⁴⁷The band-gap variation with temperature would yield extremely small changes of the band offset for the temperature range studied here.
- ⁴⁸This “flatband energy” has been calculated assuming the values $E_g^{\text{GaAs}} = 1.43$ eV for the GaAs band gap, $\Delta E_V = 0.47$ eV for the GaAs/AlAs valence-band offset, and $|E_{\text{Al}(2p)} - E_V| = 72.86$ eV for the Al(2*p*) binding energy (Ref. 8). The valence-band-offset value has been determined through PES measurements of the “apparent” valence-band offset in the GaAs/AlAs(100) heterostructure without intralayer at RT, which give $\Delta E_V^* = 0.5$ eV; in order to obtain the “real” offset, the value of the overlayer band bending (0.03 eV, calculated by solving Poisson’s equation) must be subtracted (see Ref. 15).
- ⁴⁹The kinetic energy of the Ga(3*d*) level has been calculated as-

suming the value $|E_{\text{Ga}(3d)} - E_V| = 18.86$ eV for the Ga(3*d*) binding energy (Ref. 8).

⁵⁰The small (0.08 eV) rigid shift of the Al(2*p*), Ga(3*d*) and valence-band-edge signals observed for the GaAs/Si/AlAs(100) sample upon cooling [Fig. 1(b)] might indicate that in this sample the bands are not strictly flat in the AlAs region at RT, although it could also be related with a small inhomogeneity in the pinning position of the Fermi level at the surface.

⁵¹D. Paget, B. Vinter, and D. Rondi, J. Appl. Phys. **74**, 7306 (1993).

⁵²The existence of an upward band bending at RT is deduced from the Ga(3*d*) and valence-band-edge PES data that we have obtained, which indicate that the Fermi level is pinned at the sur-

face 0.5 and 0.7 eV below the conduction-band minimum in the GaAs(110) and GaAs/Si/GaAs(110) samples, respectively. Deep in the bulk of the samples, E_F lies very close to the CBM, due to the high *n*-type doping level of the substrate.

⁵³M. Marsi, R. Houdre, A. Rudra, M. Illegems, F. Gozzo, C. Coluzza, and G. Margaritondo, Phys. Rev. B **47**, 6455 (1993).

⁵⁴R. Cimino, A. Giarante, K. Horn, and M. Pedio, Surf. Sci. **331-333**, 534 (1995).

⁵⁵R. Cimino, A. Giarante, K. Horn, and M. Pedio, J. Electron Spectrosc. Relat. Phenom. **76**, 477 (1995).

⁵⁶R. Cimino, A. Giarante, K. Horn, and M. Pedio, Europhys. Lett. **32**, 601 (1995).